Supplemental Information for Design and Characterization of DNA Strand-Displacement Circuits in Serum-Supplemented Cell Medium

Joshua Fern[1] and Rebecca Schulman[1,2]

[1]Chemical and Biomolecular Engineering, Johns Hopkins University, Baltimore, Maryland 21218; United States of America
[2]Computer Science, Johns Hopkins University, Baltimore, Maryland 21218, United States of America

Table of Contents

SI 1: Measuring the degradation of DNA circuit components

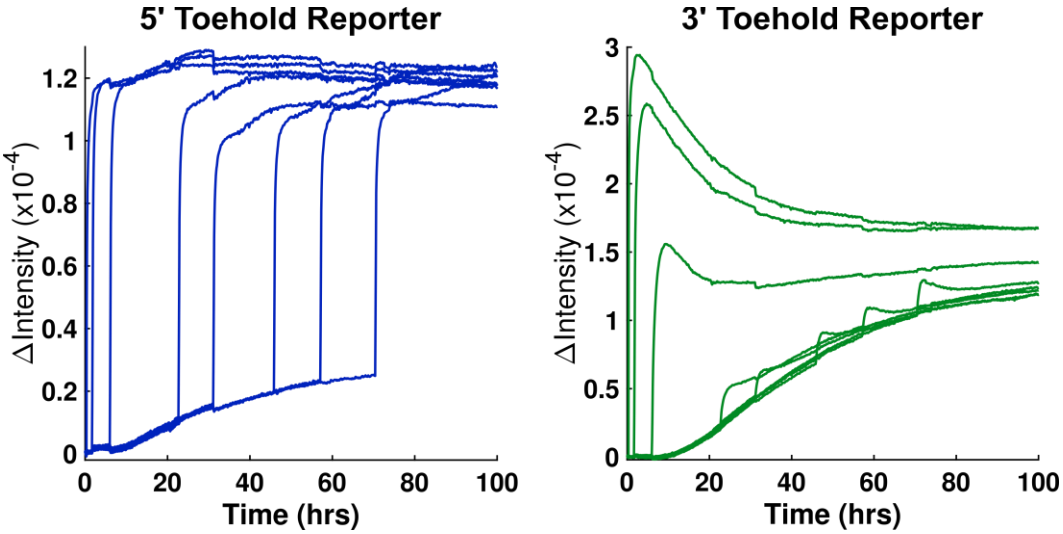

Supplemental Figure 1: Reporter complexes (200 nM), with either a 5' (*left*) or a 3' (*right*) toehold domain, were incubated in nuclease-screened medium. Output strand, with a final concentration of 250 nM, was added after 0.4, 1.8, 6.1, 22.8, 31.2, 46, 57.2, and 70.6 hours. The max intensity changes shown here are reported in Figure 2 of the Main Text. Curves are the average of two – three repeats of the same experiment performed in separate qPCR wells using the same batches of materials.

Supplemental Note 1: Calculating normalized fluorescence intensity change

In order to compare the different changes in fluorescence intensity observed by reactions with 5' and 3' toehold Reporter complexes, and to compare the changes in fluorescence intensity when the different types of Output strands (*e.g.*, 5' toehold, 3' toehold, backbone-modified) are added, the change in fluorescence intensity observed when Output and Reporter were mixed together was normalized as a function of time.

This normalized intensity, used in Figures 2, 3 and Supplemental Figure 2, was calculated using the equations:

$$Normalized\ Intensity\ = \frac{\Delta I(i)}{\Delta I(i = 0.5\ hrs)}$$

$$\Delta I(i) = Int(\ Inv.Region) - Int(Baseline)$$

where *i* represents the time point of Reporter or Output addition to incubating Output or Reporter, respectively (*e.g.*, the times listed in Supplementary Figures 1and 2). The *Baseline* is the fluorescence intensity produced from Reporter-containing solution in the absence of invading Output strand. For experiments where Reporter is incubated in NS medium, the *Baseline* is the average intensity of the measurements 20 minutes prior to adding Output strand up to the time point of Output addition. For experiments where Output was added prior to the Reporter, the *Baseline* is the average intensity of NS medium containing only Reporter over a 30 minute span immediately after Reporter was added to cell medium. The *Inv. Region* is the average intensity over the time 30 – 50 minutes after Reporter and Output are mixed together at each time point. This range was chosen as it gives enough time for Reporter and Output to react, but is before nucleases can significantly digest Reporter complexes into a disassembled state.

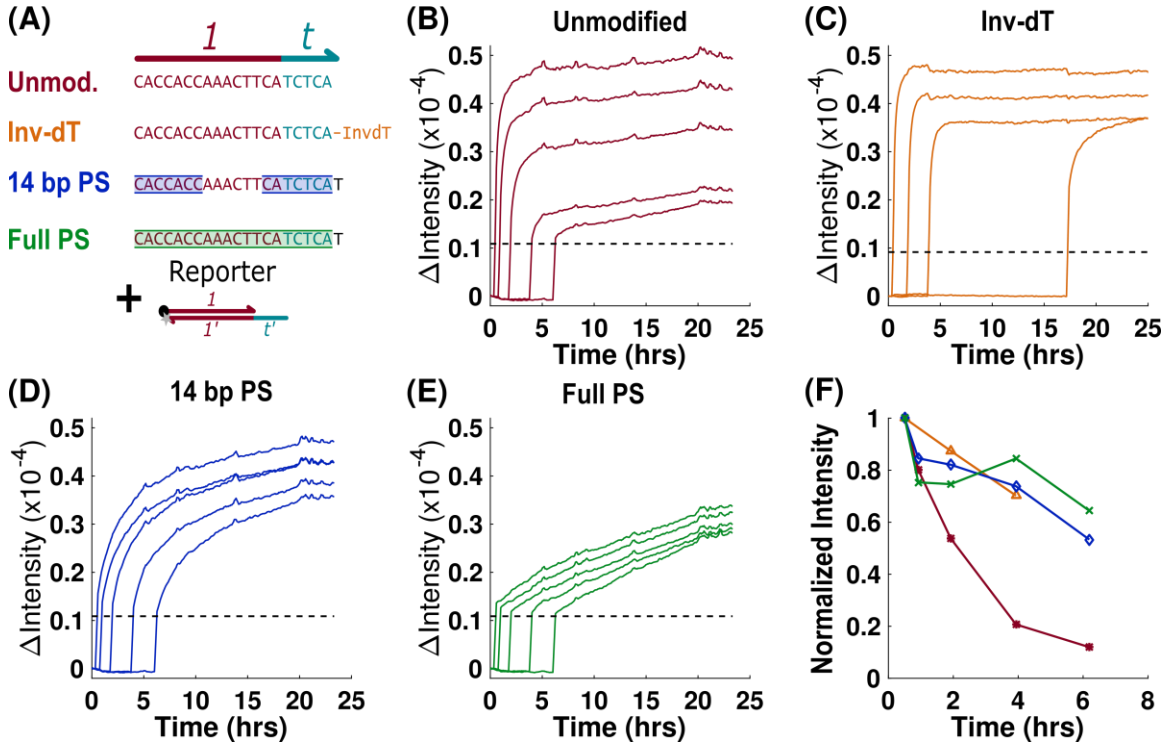

Supplemental Figure 2: Interaction of Reporter and Output strands with and without backbone or base modifications after different periods of Output strand incubation in nuclease-screened serum. (A) Schematic of unmodified, inverted thymine (Inv-dT)-modified, or phosphothiorate-modified Output strands. An Output strand was modified with an inverted dT base at the 3' end (orange text). Phosphothiorate bonds were added along the backbone of 14 nucleotides (7 each side, blue shaded regions) or along the full length of the strand (20 nucleotides, green shaded regions). A thymine base (unmodified backbone) was added to the 3' end of each phosphothiorate-modified strand due to synthesis restrictions from IDT. (B) Unmodified Output strands were incubated at 200 nM for 0.5, 1, 2, 4, or 6 hours, after which 100 nM Reporter complex was added. The major decrease in fluorescence change in samples that had been incubated for a long time as compared to shorter times implies Output strands were mostly degraded after 6 hours of incubation. (C) The experiment in (B) was repeated with the inverted dT-modified Output with the same durations of incubation, except a 17 hour timepoint was exchanged for the 6 hour timepoint. By comparison, there is just a 25% loss of response to the Reporter after 18 hours of Output incubation in serum. (D) The experiment in (B) was repeated with the Output with 14 phosphorothioate-modified nucleotides. The response to the Reporter was 40% smaller after a 6 hour incubation in serum, suggesting that about 40% of the strands were significantly degraded by that time. (E) The experiment in (B) was repeated with the Output with only phosphorothioate-modified nucleotides. Though the absolute magnitude of the response to the Reporter complex was largely unchanged after incubation in serum, the kinetics of the reaction appeared to be significantly slower than unmodified DNA, suggesting that these modifications would not allow effective strand-displacement in serum. (F) Comparison of the relative amount of degradation observed for each modified or unmodified Output species as a function of incubation time in serum, as measured by the decrease in response to the Reporter complex. The inverted dT modification and phosphorothioate backbone modifications both significantly reduce the rate of degradation, but the phosphorothioate modifications reduce the rate of strand-displacement kinetics as well. The calculation of normalized intensity is described in Supplemental Note 1.

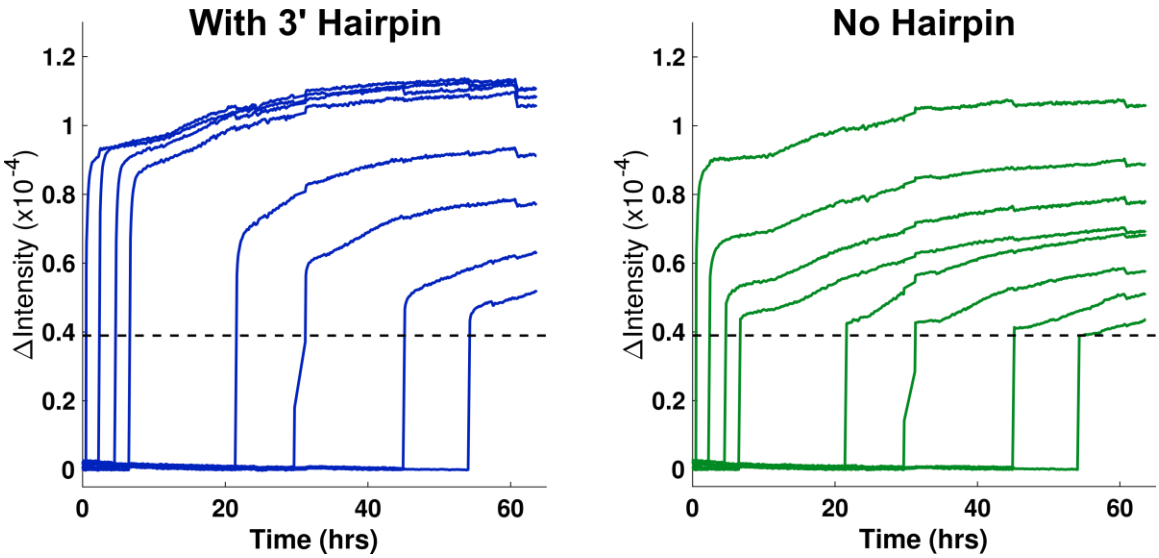

Supplemental Figure 3: Reporter complexes at 200 nM were added at various times to 100 nM Output strands, either with (*left*) or without (*right*) a 3' hairpin domain (Main Text Figure 3A), incubated in nuclease-screened medium. The intensity changes seen here are normalized and reported in Figure 3 of the Main Text. The dashed black line indicates the fluorescence intensity of 200 nM Reporter alone. Curves are the average of three repeats of the experiment.

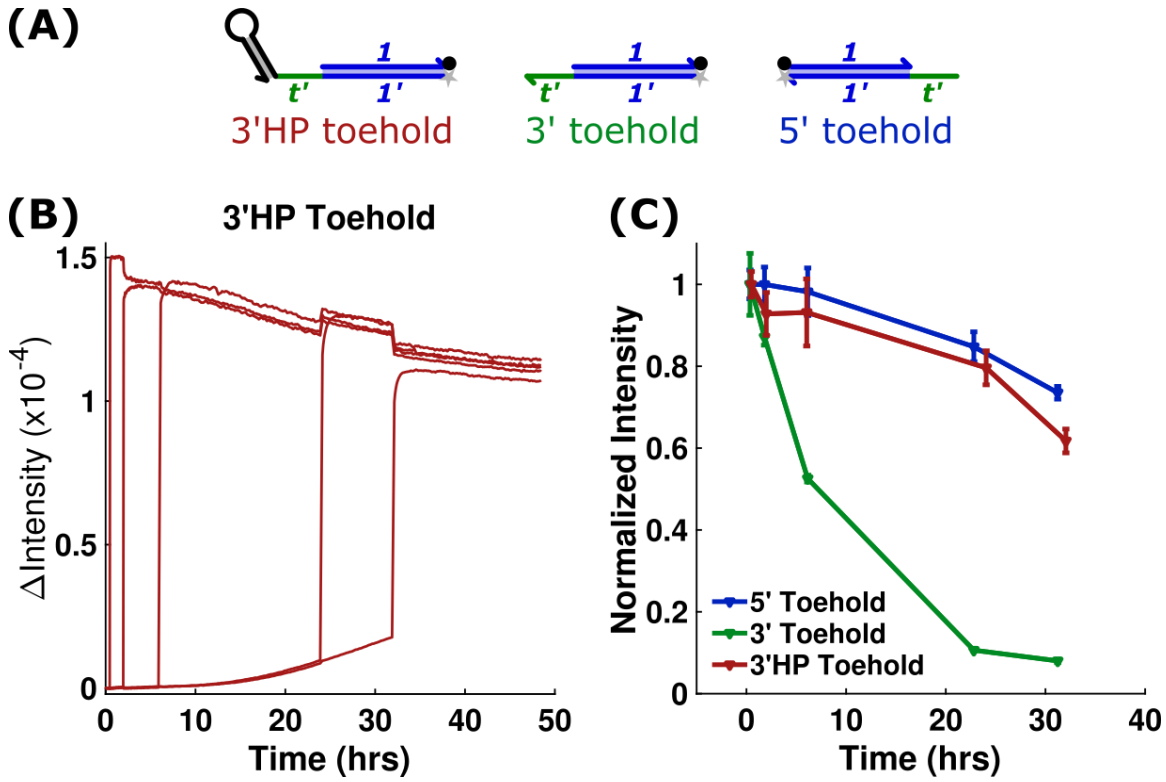

Supplemental Figure 4: The functional stability of Reporter complexes with a 3' toehold and hairpin in nuclease-screened serum-supplemented DMEM. (A) Diagram of the 3' toehold Reporter modified with a 3' hairpin and unmodified 3' and 5' toehold Reporters. (B) The change in fluorescence over time of 200 nM of the modified Reporter complexes in nuclease-screened serum-supplemented DMEM. Output strands (250 nM) were added to the Reporter complexes at 0.5, 2, 6, 24, 32 hours of incubation. Each curve is the average of either two or three repeats of the same experiment performed in separate qPCR wells using the same batches of materials. (C) The change in fluorescence upon the addition of Output plotted as a function of the Reporter's incubation time. Data for the 5' and 3' toehold Reporters in analogous experiments is copied from Figure 2 of the Main Text for comparison purposes.

Supplemental Note 2: Calibration of [Disassembled Reporter]

The fluorescence intensity change due to the dehybridization of the Reporter complex with 5' toeholds caused either by invasion by the Output strand or by nuclease digestion was converted into the concentration of Disassembled Reporter using a calibration curve that related known changes in hybridized Reporter complex to measured changes in fluorescence (Supplemental Figure 5). To build this calibration curve, Output was added to a final concentration of 50, 100, 150, 200, or 250 nM to 200 nM Reporter complexes incubated in nuclease-screened medium for 30 minutes. The change in fluorescence intensity for each sample was then calculated by subtracting the average fluorescence intensity of the sample over a 10 minute period immediately prior to Output addition from the average fluorescence intensity over a 2 hour period well after the reaction between the Output and the Reporter complex had reached completion (Supplemental Figure 5), *i.e.*:

$$\Delta Fluorescence = Avg.Intensity(t = 1.7 - 3.7\ hrs) - Avg.Intensity(t = 20 - 30\ min)$$

Based on the observed lifetime of Reporter complexes in NS medium (Main Text Figures 1 – 2), we assumed that the change in fluorescence intensity observed in these experiments was due primarily to reactions between Output strands with Reporter molecules, rather than digestion of the Reporter by nucleases. We plotted the change of fluorescence as a function of the concentration of Output that was added and used the slope of a linear fit to this plot to determine the relationship between the amount of Output added and the change in fluorescence to determine the concentration of Disassembled Reporter in our reactions using the change in fluorescence intensity.

In an ideal strand-displacement reaction, the fluorescence would reach a maximum once the concentration of Output that was added equaled the concentration of the Reporter. However, we observed that the fluorescence intensity when 250 nM of Output was mixed with 200 nM Reporter complexes was larger than the fluorescence intensity when 200 nM of Output was mixed with 200 nM of Reporter in NS medium. One potential reason for this lack of saturation could be that nucleases may bind to some reactants and make them inaccessible and thus unable to react quickly, even if they are not degraded. If more Output undergoes this process than Reporter, then we would observe that more Output than Reporter would be needed to achieve a

maximum signal. Alternatively, when the concentration of Output is close to or exceeds the concentration of Reporter, virtually all Reporter must react in order to reach the expected equilibrium state. The approach to the equilibrium state may thus be limited by partially digested Reporters with shorter toeholds.

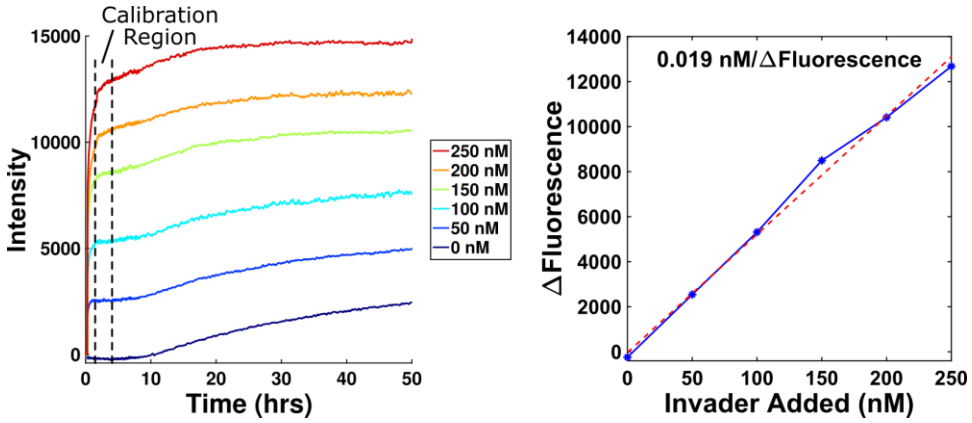

Supplemental Figure 5: Converting the change in fluorescence intensity into [Disassembled Reporter]. The change in fluorescence in the *right* plot was calculated by subtracting the average intensity of the solution prior to Output invader addition from the average intensity of each curve in the Calibration region (*left*). The Reporter concentration is 200 nM.

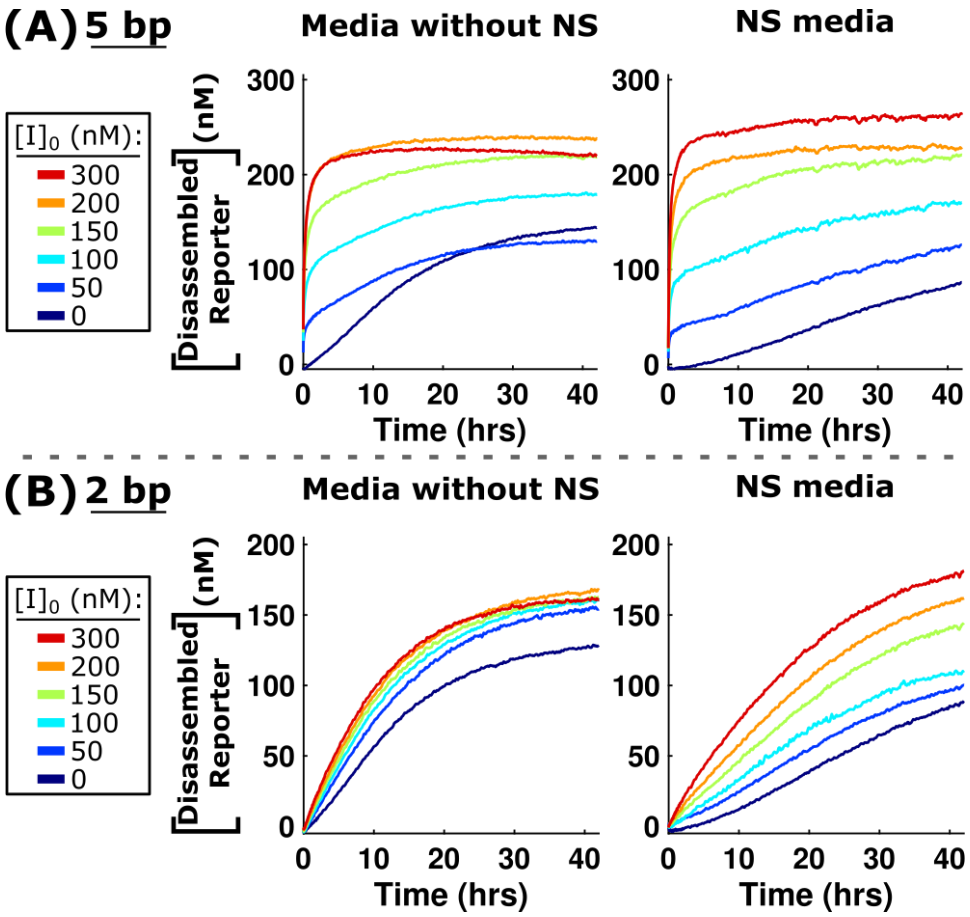

Supplemental Figure 6: Release reactions conducted in serum-supplemented medium without nuclease-screening components (*left*) compared with the same experiments performed in NS medium (*right*). The Reporter and Source concentrations are 200 nM. The data shown for NS medium is the same as in Figure 5 of the Main Text.

SI 2: Modeling DNA strand-displacement in serum

In order to understand and predict the dynamics of the strand-displacement reactions in the presence of interfering and digesting enzymes (*e.g.*, nucleases), we generated a model that incorporates both the strand-displacement reactions and the reactions between the nucleases and the added DNA circuit components. The model also includes reactions between the nucleases and the inhibitor and screening molecules in the nuclease-screened medium that we developed.

In general, the conversion of a substrate to product using an enzyme catalyst was modeled using the standard enzyme reaction model:

$$Substrate + Enzyme \rightleftharpoons Enzyme{:}Substrate \rightarrow Enzyme + Product \qquad (1)$$

where the *Substrate* is either a nuclease inhibitor (*i.e.*, actin or competitor DNA) or DNA circuit component, and *Enzyme:Substrate* indicates an enzyme-bound substrate intermediate complex. Here, we layout the reactions and data that was fit to obtain the figures in the main text and the estimated reaction rate constants and component concentrations.

All fitting and simulations were conducted using MATLAB's built-in functions *lsqnonlin*, *nlpredci*, and *nlparci*: standard tools for non-linear regression. Confidence intervals on fitted parameters were calculated using *nlparci*, and *nlpredci* was used to calculate 95% confidence intervals on the model predictions. For all reactions involving enzymes, the initial guess of the reaction rate constant was 0.5 1/M-sec for bimolecular reactions or 0.5 1/sec for unimolecular reactions.

As seen in Supplemental Tables 1 – 6, the initial concentration of some reaction components used in fitting the reaction rate constants, Inhibitor concentrations, and nuclease concentrations were adjusted in order to obtain more sensible parameter fits. The changes that were made presumably reflected experimental variation in pipetting. Additionally, the fluorescence of the reaction mixtures usually increased beyond the expected limit that should be observed from 200 nM Output reacting with 200 nM of Reporter, and there was no way for the model to account for this discrepancy through a choice of reaction rates (Supplemental Note 2). We therefore accounted for this phenomenon in the simulations by adjusting the effective Reporter concentration of each reaction mixture. Due to this adjustment and the fact that the effective concentrations of Inhibitors and Enzymes are unknown, the reaction rate constants for all

reactions involving enzymes should be viewed as predictive estimates relative to the assumed concentrations in each experiment below.

SI 2.1: Reporting reaction

We began to develop the model using a simple system containing only the Output and the Reporter complex. We used this process to fit the reactions between Output strands and the Reporter complex, the interactions between each component and nucleases, and between the nuclease inhibitors and nucleases in the nuclease-screened medium. We used a system in which the Output binds to the Reporter *via* a 5 base-pair toehold that initiates the strand-displacement process (Main Text Figure 1A). Since there is only a 0 bp toehold on the other side of the complex, this reaction is assumed to be irreversible due to the ~10^5-fold higher forward reaction rate constant.

$$Output + Reporter \xrightarrow{k_{Reporter}} Fluorophore + Quencher \quad (2)$$

To account for the reactions between the Reporter and the nucleases present in serum-supplemented medium, we built a model in which nucleases bind to the Reporter complex and produce a degraded product that is a semi-stable, partial Reporter complex. Partial Reporter complexes can be further digested to a fully disassembled state. We developed this model based on observations of changes in fluorescence of Reporter complexes when the Reporter is added to serum-supplemented medium. An increase in fluorescence, which in the absence of invading Output would be driven by irreversible separation of the FAM and the quencher on the complementary strand, was not immediate and constant. Instead, fluorescence increase occurred with sigmoidal-like dynamics. The delayed onset of fluorescence increase could be caused by a need for multiple rounds of degradation of the Reporter complex to occur before the FAM molecules and the quencher on its complement are no longer co-localized by hybridization. This is sensible because degradation would have to occur close to the FAM-modified termini for the remaining DNA strand to melt off the complex, resulting in a free and active FAM molecule. This multi-step process of degradation is modeled using the following reactions:

$$Reporter + Enzyme \xrightarrow{k_{ERf}} Reporter{:}\,Enzyme \quad (3)$$

$$Reporter{:}\,Enzyme \xrightarrow{k_{ERrev}} Reporter + Enzyme \quad (4)$$

$$Reporter{:}\,Enzyme \xrightarrow{k_{ERDeg}} Enzyme + Rep_{Partial} \quad (5)$$

$$Rep_{Partial} + Enzyme \xrightarrow{k_{ERf}} Rep_{partial}{:}\,Enzyme \quad (6)$$

$$Rep_{partial}{:}\,Enzyme \xrightarrow{k_{ERrev}} Rep_{partial} + Enzyme \quad (7)$$

$$Rep_{partial}{:}\,Enzyme \xrightarrow{k_{ERDeg}} Enzyme + Fluorophore + Quencher \quad (8)$$

$$Output + Rep_{partial} \xrightarrow{k_{Reporter}} Fluorophore + Quencher \quad (9)$$

where $Rep_{partial}$ is a partially degraded Reporter complex with the fluorophore in a quenched state. Because the reactions in equations 6 – 8 are based upon the same general reaction progression as in equations 3 – 5, and to reduce the total number of fitted reaction rate constants, the reactions in equations 6 – 8 were assumed to have the same reaction rate constant as their corresponding reaction in equations 3 – 5 (*e.g.*, equation 3 and 6 have the same reaction rate constant). Equation 9 represents the capability of Output strands to bind to partially degraded Reporter complexes and was assumed to have the same reaction rate constant as non-degraded Reporter (equation 2). We neglected interactions between Output strands and nucleases in cases where Output strands are added to incubated Reporters because the timescale of single-stranded degradation in nuclease-screened medium appeared significantly slower than the timescale for the Reporter-Output reaction to reach completion (*i.e.*, all Output strands bind and react with Reporter complexes). This reaction runs to completion in practice in 2 – 3 hours (Supplemental Figure 5), whereas Outputs with 3' hairpins are resistant to degradation over 6 hours (Main Text Figure 3B, Supplementary Figure 3).

To account for the effects of nuclease inhibitors in the nuclease-screened medium, we included reactions in which the enzymes (*i.e.*, nucleases) interacted with the inhibitors:

$$Inhibitor + Enzyme \xrightarrow{k_{EIf}} Enzyme{:}\,Inhibitor \quad (10)$$

$$Enzyme{:}\,Inhibitor \xrightarrow{k_{EIrev}} Enzyme + Inhibitor \quad (11)$$

$$Enzyme{:}\,Inhibitor \xrightarrow{k_{EIDeg}} Enzyme + Waste \quad (12)$$

Here, all inhibitors were lumped into a class of composite reactions for simplicity because the exact, combined effects of the actin protein and the inert DNA strands on nuclease activity in nuclease-screened serum-supplemented medium are unknown. While reaction rate constants for some of these reactions involving specific nucleases (*e.g.*, DNaseI) have previously been measured for models implementing the Michaelis-Menten approximation,[1,2,3] it was assumed that the varying and unknown types, and concentrations, of nuclease subtypes within fetal bovine serum, and the complexity of inhibitor types used, precluded the use of such an approximation and corresponding parameters.

The reaction rate constants for the above reactions (equations 2 – 12) and the concentrations of the Inhibitors and Enzymes were fit using the measured kinetics of the Reporter and Output strands in nuclease-screened medium (Supplemental Figure 5, fits shown in Supplementary Figure 7). The fitted rate constants and concentrations are listed in Supplemental Table 1. These reaction rate constants and Enzyme/Inhibitor concentrations were assumed in fitting further experiments in order to expand the model.

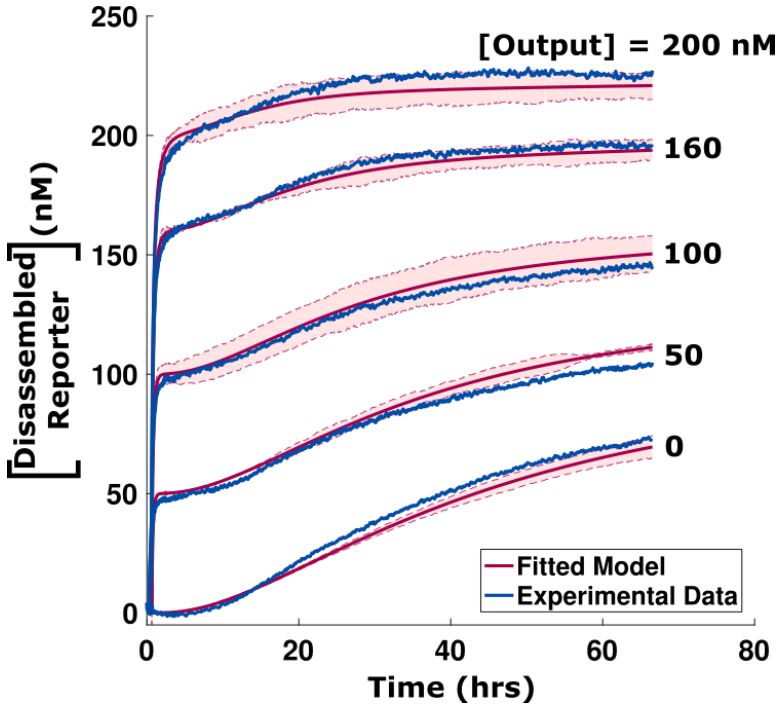

Supplemental Figure 7: Experimental characterization of the change in fluorescence when Reporter (5 nucleotides, 5' toehold) complexes and Output strands are combined in nuclease-screened medium (same data as in Supplemental Figure 5) and fitted using the model described in SI 2.1 with parameters as given in Supplemental Table 1. Output concentrations listed are the simulated concentrations. Shaded red regions show the range of values predicted with 95% confidence.

Supplemental Table 1: List of parameters used for fitting the model for the irreversible reporter in nuclease-screened medium and the calculated fitted parameters. Parameters are listed as the fitted value +/- their 95% confidence interval in parentheses. Some constants have large error values. This large range of valid parameters may be caused by the fact that varying these rates does not vary the outcome significantly. For example, the model appears to fit the data for a wide range of values of k_{ERrev}, so long as it is smaller than the rate of degradation, *i.e.*, most substrate that binds to a nuclease is degraded. We observed that the model did not work well without including these parameters and reactions.

Reaction Component	Expt. Conc. (nM)	Modeled Conc. (nM)	Rate Constant	Fitted Parameter
Reporter	200	250	$k_{Reporter}$ (1/M-sec)	$8.5(0.2)\text{x}10^{3}$
Output	0, 50, 100, 150, 200	0, 50, 100, 160, 200	k_{ERf} (1/M-sec)	$7(3)\text{x}10^{3}$
Enzyme		31.3	k_{ERrev} (1/sec)	$4(2\text{x}10^{9})\text{x}10^{-14}$
Inhibitor		620	k_{ERDeg} (1/sec)	$8.6(0.8)\text{x}10^{-5}$
			k_{Elf} (1/M-sec)	$3(1.5)\text{x}10^{2}$
			k_{Elrev} (1/sec)	$5(1000)\text{x}10^{-7}$
			k_{ElDeg} (1/sec)	$2(1\text{x}10^{7})\text{x}10^{-11}$

SI 2.2: Single-stranded DNA degradation

In addition to DNA complexes, the single-stranded DNA components are also susceptible to degradation by nucleases. This effect is observed in Supplemental Figure 2 and was one of the primary influencers in the choice of strand design, especially the hairpin domain added to the 3' termini of all circuit strands expected to be in a single-stranded form (*i.e.*, Output and Initiator strands). To attempt to quantify the rate and degree of degradation of Output strands with 3' hairpin domains due to nucleases for these DNA strand-displacement circuits, we used the data shown in Supplemental Figure 3, the reactions in equations 2 – 12 and the parameters and concentrations in Supplemental Table 1 to fit the rates for the following reactions:

$$Output + Enzyme \xrightarrow{k_{EssDNAf}} Output{:}\,Enzyme \tag{13}$$

$$Output{:}\,Enzyme \xrightarrow{k_{EssDNArev}} Output + Enzyme \tag{14}$$

$$Output{:}\,Enzyme \xrightarrow{k_{EssDNADeg}} Enzyme + Waste \tag{15}$$

The parameters that were fit are show in Supplemental Table 2 and the use of these fits to model the process is shown in Supplemental Figure 8. Although the confidence intervals for the fit parameters are quite small, the overall fit to the experimental data shows significant deviation

between experiment and model for long Output strand incubation times, especially at 45 and 55 hours. Re-fitting the Reporter-Enzyme reactions concurrently with the Output-Enzyme reactions did not provide an improved fit to the data at long times. The lack of agreement between the model and the data here indicate that there are further interactions occurring in the experiment that we have not accounted for with the model.

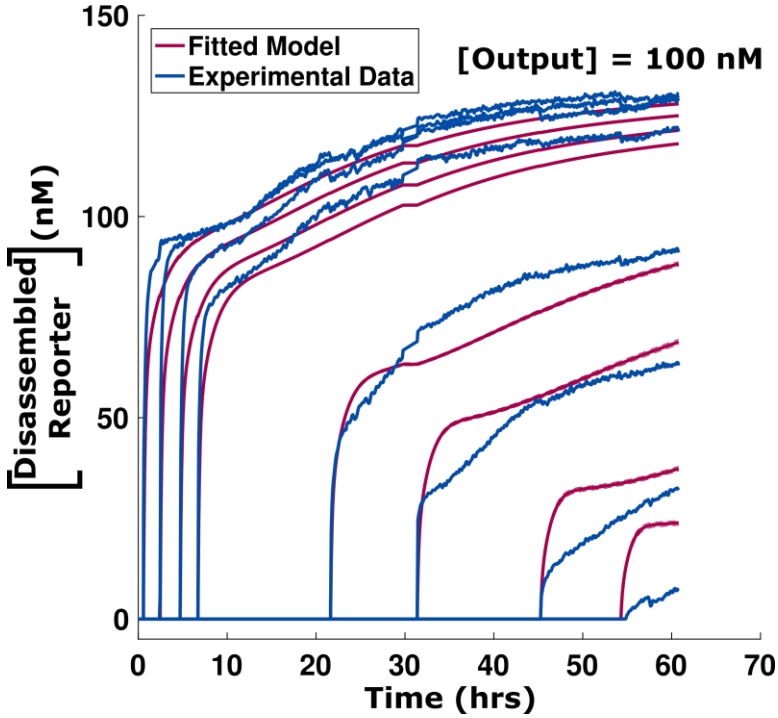

Supplemental Figure 8: The predictions of our model for how Output strands respond to the Reporter complex after the Output is incubated in nuclease-screened medium for different times. Reporter complexes at 200 nM were added at various times to 100 nM Output strands that contained a 3' hairpin domain. The fitted model has parameters determined as described in Supplemental Sections 2.1 – 2.2. Confidence intervals (95%) for the fit are too small to be observed. Fitted reaction rate constants and modeled concentrations are listed in Supplemental Table 2. One limitation of our model is that there is only one rate at which the Output and Reporter can react, even if the Reporter or Output are partially degraded. The model is therefore unable to fit cases where the concentration of disassembled Reporter slowly rises due to a slow reaction rate between partial Output and Reporters.

Supplemental Table 2: List of fit values for the parameters for the model for the degradation of single-stranded DNA components in serum-supplemented medium as described in Supplemental Section 2.2 using the data shown in Supplemental Figure 8. Parameters are listed as the fitted value +/- their 95% confidence interval in parentheses.

Reaction Component	Expt. Conc. (nM)	Modeled Conc. (nM)	Rate Constant	Fitted Parameter
Reporter	200	200	$k_{EssDNAf}$ (1/M-sec)	$1.69(0.07)\times10^{7}$
Output	100	100	$k_{EssDNArev}$ (1/sec)	$9.0(0.8)\times10^{-3}$
Enzyme		31.3	$k_{EssDNADeg}$ (1/sec)	$1.64(0.02)\times10^{-5}$
Inhibitor		620		

SI 2.3: Release reactions

We used the model developed in Supplemental Sections SI 2.1 – 2.2 as a basis for predicting and fitting more complex strand-displacement systems for use in serum and the nuclease-screened medium we developed. In standard buffers, such as TAE supplemented with Mg^{2+}, the rate constants for toehold mediated strand-displacement processes, such as the Release reaction (Main Text Figure 4) are determined primarily by the length of the toehold domain of the Source complex.[4] In TAE/Mg^{2+}, the reaction rate constant increases by a factor of 10 for each base added to the toehold for toehold lengths less than 7 bases. To determine whether this rule-of-thumb applies to DNA strand-displacement reactions conducted in serum-supplemented medium and at 37 °C, we fit rate constants for strand-displacement processes between a Source complex and Initiator strand (Main Text Figure 4) involving toeholds of 0, 2, and 5 base pairs on the Source complex. The release of Output strand was monitored using the fluorescence of an irreversible reporter (Main Text Figure 4). The degradation of the Source complex was modeled in a fashion similar to the degradation of the Reporter complex – degradation was assumed to occur in multiple stages. For simplicity, we assumed that the reaction rate constants governing the nuclease-driven degradation of the Source and partial Source complexes were the same, so that reaction rate constants for equations 17 – 18 and 21 – 22 were the same. Degradation of the single-stranded Initiator was likewise assumed to be governed by equations 25 – 27, which are analogous to equations 13 – 15 and were assumed to have the same rate constants fit for equations 13 and 15 in Supplemental Section 2.2.

$$Source + Initiator \xrightarrow{kSInit} Output + Waste \tag{16}$$

$$Source + Enzyme \xrightarrow{k_{ESf}} Source{:}\,Enzyme \tag{17}$$

$$Source{:}\,Enzyme \xrightarrow{k_{ESrev}} Source + Enzyme \tag{18}$$

$$Source{:}\,Enzyme \xrightarrow{k_{ESDPart}} Enzyme + Source_{partial} \tag{19}$$

$$Source_{partial} + Initiator \xrightarrow{kS_{Part}Init} Output + Waste \tag{20}$$

$$Source_{partial} + Enzyme \xrightarrow{k_{ESf}} Source_{partial}{:}\,Enzyme \quad (21)$$

$$Source_{partial}{:}\,Enzyme \xrightarrow{k_{ESrev}} Source_{partial} + Enzyme \quad (22)$$

$$Source_{partial}{:}\,Enzyme \xrightarrow{k_{ESDeg}} Enzyme + Output \quad (23)$$

$$Source_{partial}{:}\,Enzyme \xrightarrow{k_{ESDeg}} Enzyme + Waste \quad (24)$$

$$Initiator + Enzyme \xrightarrow{k_{EssDNAf}} Initiator{:}\,Enzyme \quad (25)$$

$$Initiator{:}\,Enzyme \xrightarrow{k_{EInitrev}} Initiator + Enzyme \quad (26)$$

$$Initiator{:}\,Enzyme \xrightarrow{k_{EssDNADeg}} Enzyme + Waste \quad (27)$$

Finally, the degradation of the Source complex (rather than reaction with the Initiator) could release the Output which could then react with a Reporter complex. Equations 23 and 24 determine how much active Output strand is produced from degraded Source complexes. An active Output strand contains a contiguous to mostly contiguous toehold and domain (complementary to the Reporter) and is able to conduct strand-displacement reactions with the Reporter complex. Based upon the observation that Source complexes (mixed with Reporter) in the absence of Initiator strand showed a delayed increase in fluorescence (Supplemental Figures 9 – 12), we modeled the degradation of Source complexes as a two-step process. Equations 2 – 15 were also included in the model, but were not fit, and the reaction rate constants for those reactions were set to their previously fit values (Supplemental Tables 1 and 2). The degradation of Initiator strands was assumed to occur with the same model and reaction rate constants as Output strands (equations 25 – 27), except the Enzyme-Initiator unbinding reaction, which was fit individually for each Source complex.

Poorly synthesized or assembled Source complexes with 0 bp toeholds could in principle interact directly with the Reporter complex at rates comparable to their reaction with the Initiator, as observed in similar reactions in nuclease-free buffers.[5] Thus, our model of 0 bp strand-displacement between the Source and Initiator also included two additional reactions to reflect this possibility.[5]

$$Source_{Leak} + Reporter \xrightarrow{kS_{Leak}R} Fluorophore + Quencher \quad (28)$$

$$Source_{Leak} + Initiator \xrightarrow{kS_{Leak}I} Output + Waste \quad (29)$$

where $Source_{Leak}$ represents Source complexes that are partially formed or have mismatches, due to synthesis or annealing errors, that enable it to react with Reporter complexes in the absence of Initiator strands. The reaction rate constants $kS_{Leak}R$ and $kS_{Leak}I$ were assumed to be 5.5×10^3 1/M-sec and 5 1/M-sec which represent ~4 bp and 1 bp toeholds, respectively.[5] The concentration of $Source_{Leak}$ was assumed to be 4% of the total initial Source concentration, Equation 28 only influences the level of fluorescence/Output detected by the Reporter prior to the addition of Initiator or prior to nucleases beginning to significantly degrade Source complexes (*e.g.*, within 6 hours of Source addition to the reaction mixture). Equation 29 directs the initial slope of the curves immediately after Initiator is added because Initiator presumably reacts with $Source_{Leak}$ 10-fold faster than with Source complexes. The reactions between $Source_{Leak}$ complexes and nucleases were not included in our model because the $Source_{Leak}$ complexes were assumed to be depleted *via* the reactions shown in equations 28 and 29 before significant degradation of $Source_{Leak}$ complexes occurs.

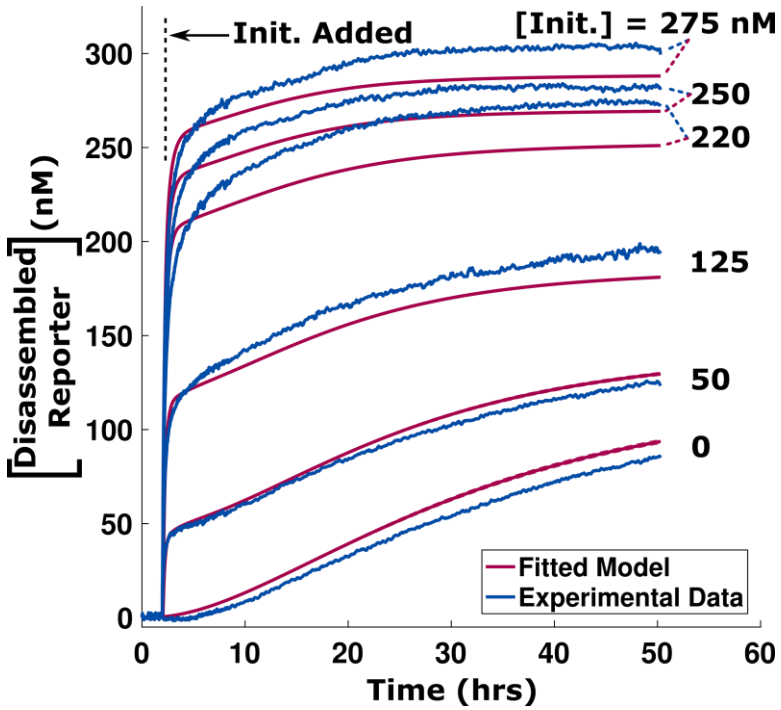

Supplemental Figure 9: Model predictions and experimental data for a system in which the Source complex can react with an Initiator strand using a 5 base pair toehold to release an Output strand. The Output strand can displace the quencher-containing strand from the Reporter complex to increase the measured fluorescence. The process and resulting parameters, including those that govern the speed of 5 base pair toehold-mediated strand-displacement in nuclease-screened medium, are given in Supplemental Section 2.3 and Supplemental Table 3. The model kinetics are predicted [Disassembled Reporter] values. Confidence intervals (95%) for the fit are too small to be observed.

Supplemental Table 3: List of fit values for the parameters for our model of strand-displacement of a Source complex by an Initiator given a 5 base pair toehold (see Supplemental Section 2.3). Data used for fitting and results are shown in Supplemental Figure 9. Parameters are listed as the fitted value +/- their 95% confidence interval in parentheses.

Reaction Component	Expt. Conc. (nM)	Modeled Conc. (nM)	Rate Constant	Fitted Parameter
Reporter	200	200, 200, 220, 280, 290, 310	k_{SInit} (1/M-sec)	7(1)x10^{4}
Initiator	0, 50, 100, 150, 200, 300	0, 50, 125, 220, 250, 275	$k_{SpartInit}$ (1/M-sec)	4(2)x10^{4}
Source (5bp)	200	275	k_{ESf} (1/M-sec)	4(2)x10^{4}
Enzyme		31.3	k_{ESrev} (1/sec)	2.2(0.3)x10^{-1}
Inhibitor		620	k_{ESDeg} (1/sec)	4(3)x10^{-2}
			$k_{EInitrev}$ (1/sec)	3(4)x10^{-2}

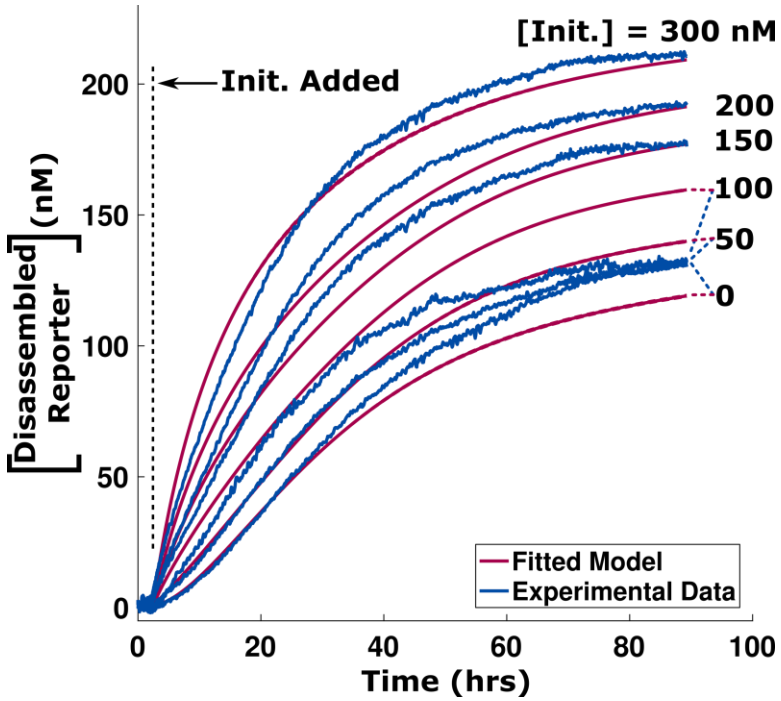

Supplemental Figure 10: Model predictions and experimental data for a system in which the Source complex can react with an Initiator strand using a 2 base pair toehold to release an Output strand. The Output strand can displace the quencher-containing strand from the Reporter complex to increase the measured fluorescence. The fitting process and resulting parameters, including those that govern the speed of 2 base pair toehold-mediated strand-displacement in nuclease-screened medium, are given in Supplemental Section 2.3 and Supplemental Table 4. The model kinetics are predicted [Disassembled Reporter] values. Confidence intervals (95%) for the fit are too small to be observed.

Supplemental Table 4: List of fit values for the parameters for our model of strand-displacement of a Source complex by an Initiator given a 2 base pair toehold (see Supplemental Section 2.3). Data used for fitting and results are shown in Supplemental Figure 10. Parameters are listed as the fitted value +/- their 95% confidence interval in parentheses.

Reaction Component	Expt. Conc. (nM)	Modeled Conc. (nM)	Rate Constant	Fitted Parameter
Reporter	200	225	k_{SInit} (1/M-sec)	$6.5(0.3)\text{x}10^{1}$
Initiator	0, 50, 100, 150, 200, 300	0, 50, 100, 150, 200, 300	$k_{SpartInit}$ (1/M-sec)	$1.5(0.5)\text{x}10^{2}$
Source (2bp)	200	220	k_{ESf} (1/M-sec)	$1.5(1.2)\text{x}10^{4}$
Enzyme		31.3	k_{ESrev} (1/sec)	$2.1(1.5)\text{x}10^{-2}$
Inhibitor		620	k_{ESDeg} (1/sec)	$2.6(4.8)\text{x}10^{-2}$
			$k_{EInitrev}$ (1/sec)	$5.1(0.7)\text{x}10^{-2}$

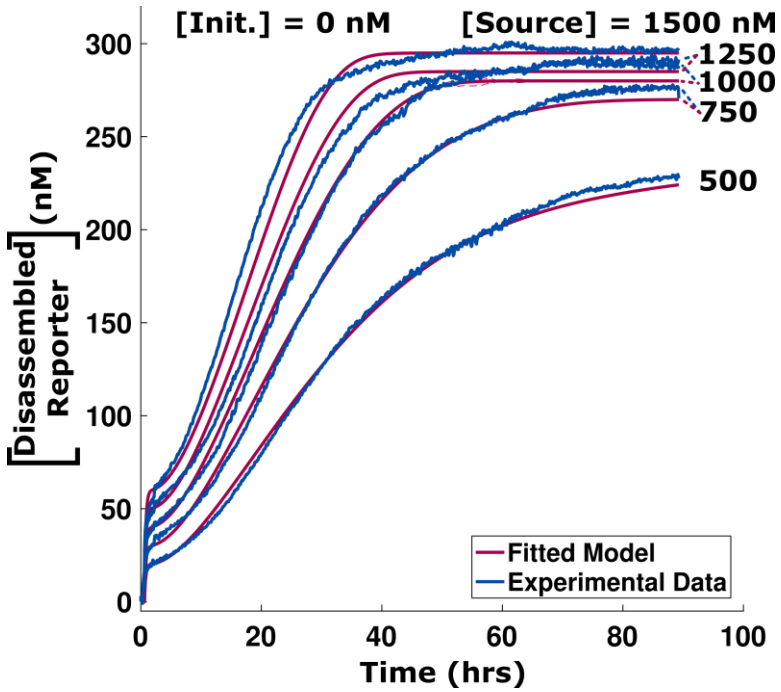

Supplemental Figure 11: Model predictions and experimental data for a system in which the 0 bp toehold Source complex can be digested by nucleases in the absence of Initiator to release an Output strand. The Output strand can displace the quencher-containing strand from the Reporter complex to change the fluorescence. The process and resulting parameters, including those that govern the speed of 0 base pair toehold-mediated strand-displacement in nuclease-screened medium, are given in Supplemental Section 2.3 and Supplemental Table 5. The model kinetics are predicted [Disassembled Reporter] values. Confidence intervals (95%) for the fit are too small to be observed.

Supplemental Table 5: List of fit values for the parameters for our model of nuclease-0 bp toehold Source complex reactions in the absence of Initiator (see Supplemental Section 2.3). Reaction components with multiple modeling concentrations are listed in order in regards to the other components (*e.g.*, [Reporter]=270 nM and [Source]=500 nM are initial concentrations for one set of modeled reaction mixtures). Data used for fitting and results are shown in Supplemental Figure 11. Parameters are listed as the fitted value +/- their 95% confidence interval in parentheses.

Reaction Component	Expt. Conc. (nM)	Modeled Conc. (nM)	Rate Constant	Fitted Parameter
Reporter	200	270, 270, 280, 285, 295	k_{ESf} (1/M-sec)	$1.2(0.3)\text{x}10^{4}$
Initiator	0	0	k_{ESrev} (1/sec)	$5(100)\text{x}10^{-5}$
Source	500, 750, 1000, 1250, 1500	500, 750, 1000, 1250, 1500	k_{ESDeg} (1/sec)	$3.1(0.2)\text{x}10^{-3}$
Enzyme		31.3		
Inhibitor		620		

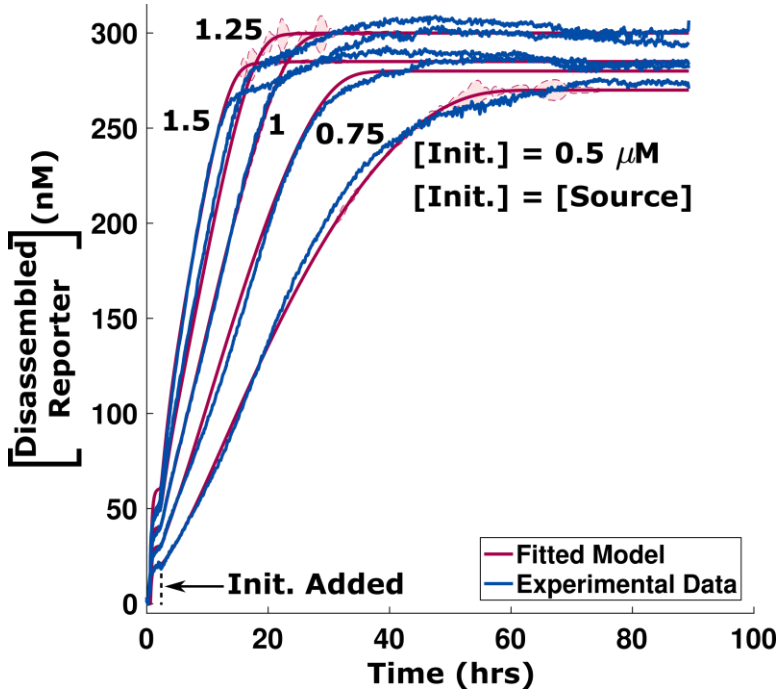

Supplemental Figure 12: Model predictions and experimental data for a system in which the Source complex can react with an Initiator strand using a 0 base pair toehold to release an Output strand. The Output strand can displace the quencher-containing strand from the Reporter complex to increase the measured fluorescence. The process and resulting parameters, including those that govern the speed of 0 base pair toehold-mediated strand-displacement in nuclease-screened medium, are given in Supplemental Section 2.3 and Supplemental Table 6. The model kinetics are predicted [Disassembled Reporter] values. Confidence intervals (95%) for the fit are too small to be observed.

Supplemental Table 6: List of fit values for the parameters for our model of strand-displacement of a Source complex by an Initiator given a 0 base pair toehold (see Supplemental Section 2.3). Reaction components with multiple modeling concentrations are listed in order in regards to the other components (*e.g.*, [Reporter]=270 nM and [Source]=500 nM are initial concentrations for one set of modeled reaction mixtures). Data used for fitting and results are shown in Supplemental Figure 12. Parameters are listed as the fitted value +/- their 95% confidence interval in parentheses.

Reaction Component	Expt. Conc. (nM)	Modeled Conc. (nM)	Rate Constant	Fitted Parameter
Reporter	200	270, 280, 300, 300, 285	k_{SInit} (1/M-sec)	$9(1)\text{x}10^{-1}$
Initiator	500, 750, 1000, 1250, 1500	500, 750, 1000, 1250, 1500	$k_{SpartInit}$ (1/M-sec)	$9.3(0.7)\text{x}10^{1}$
Source	500, 750, 1000, 1250, 1500	500, 750, 1000, 1250, 1500	k_{ESf} (1/M-sec)	$6(6)\text{x}10^{3}$
Enzyme		31.3	k_{ESrev} (1/sec)	$2(200)\text{x}10^{-4}$
Inhibitor		620	k_{ESDeg} (1/sec)	$2(3)\text{x}10^{-2}$
			$k_{EInitrev}$ (1/sec)	1.3(0.1)

SI 3: Predicting the behavior of complex DNA strand-displacement circuits

Complex strand-displacement circuits could make it possible to integrate information about the concentrations of different molecules and direct multi-faceted responses with controlled responses in serum. To design such complex circuits, tools for predicting their behavior in advance will be needed. In this section, we use our experimental characterization of DNA strand-displacement reactions to predict the behavior of multi-stage reaction cascades and a timer to work toward building models of these systems, and to determine what changes will be needed in order to build reliably robust circuits of these types. The models we construct build on the model introduced in SI 2.

SI 3.1: Multi-layer cascade circuit simulations

To model the kinetics of a strand-displacement cascade with multiple Sources and Initiators (Main Text Figure 6), we expanded the model presented in SI 2 with strand-displacement reactions between the additional components and reactions that modeled their degradation. Each layer of the cascade is modeled by a set of reactions like those for the first layer, *i.e.*, equations 16 – 27. Additional reactions allow partially degraded Source complexes to release Initiator strands that can signal the next layer of the cascade, analogous to the reaction shown in equation 23. The resulting set of equations involving either the Source or Initiator or their partially degraded versions of these species in an n-layer circuit are therefore:

$$Source_n + Initiator_n \xrightarrow{kSInit} Initiator_{n-1} + Waste \tag{30}$$

$$\vdots$$
$$\vdots\ n - circuit\ layers$$
$$\vdots$$

$$Source_1 + Initiator_1 \xrightarrow{kSInit} Output + Waste \tag{31}$$

$$Source_n + Enzyme \xrightarrow{k_{ESf}} Source_n{:}\,Enzyme \tag{32}$$

$$Source_n{:}\,Enzyme \xrightarrow{k_{ESrev}} Source_n + Enzyme \tag{33}$$

$$Source_n{:}\,Enzyme \xrightarrow{k_{ESDPart}} Enzyme + Source_{n_{partial}} \tag{34}$$

$$Source_{n_{partial}} + Initiator \xrightarrow{kS_{Part}Init} Initiator_{n-1} + Waste \quad (35)$$

$$Source_{n_{partial}} + Enzyme \xrightarrow{k_{ESf}} Source_{n_{partial}}: Enzyme \quad (36)$$

$$Source_{n_{partial}}: Enzyme \xrightarrow{k_{ESrev}} Source_{n_{partial}} + Enzyme \quad (37)$$

$$Source_{n_{partial}}: Enzyme \xrightarrow{k_{ESDeg}} Enzyme + Initiator_{n-1} \quad (38)$$

$$Source_{n_{partial}}: Enzyme \xrightarrow{k_{ESDeg}} Enzyme + Waste \quad (39)$$

where *n* indicates the layer number of the cascade circuit. For example, in a 2-layer cascade, $Initiator_2$ and $Source_2$ react to release $Initiator_1$ (equation 30). $Initiator_1$ can then react with $Source_1$ to release the Output strand (equation 31). Parameters for the above reactions were taken from Supplemental Tables 1 – 6 above. Degradation and DNA strand-displacement reaction rate constants for Source complexes were chosen based upon the toehold length (*e.g.*, Source with a 5 bp toehold was simulated with parameters from Supplemental Table 3). As described in SI 2, there was a discrepancy between the simulated concentrations and the experimental concentrations of reaction components that generated the best fit to the data. Along the lines of generating the best prediction for experimentally derived data, we simulated the cascade system with 250 nM of Reporter complexes, which may be assumed to experimentally match a Reporter concentration of 200 nM as demonstrated in SI 2. Source complexes were assumed to have matching experimental and simulation concentrations since the variance was only detected in the 2 bp and 5 bp toehold Release reaction cases shown in SI 2.

Supplemental Table 7: List of concentrations used for simulating the reaction between Initiator and Source complexes in the 2-layer cascade reaction systems incubated in nuclease-screened medium.

Reaction Component	Modeled Conc. (nM)	Expected Expt. Conc. (nM)
Reporter	250	200
$Initiator_2$	0, 50, 100, 150, 200, 300	0, 50, 100, 150, 200, 300
$Source_1$ = $Source_2$	200	200

We used this model to predict the kinetics of a 2-layer strand displacement cascade with toehold lengths of 5 bp or 2 bp for both layers, as well a cascade with 2 layers with toehold lengths of 5 and 2 bp for the 2nd and 1st layer of the circuit. To understand the kinetics of the

cascade, we began by simulating these two-level cascade circuits in the absence of nucleases (*e.g.*, serum-free medium) in order to compare the effect of toehold length in the multi-layer circuits (Supplemental Figure 13). In this case, all nuclease-dependent reactions are omitted from the model and the reaction rate constants for the remaining reactions were taken from Supplemental Tables 1 – 6. In this serum-free case, the varying input Initiator concentrations were clearly distinguishable from one another.

Simulation of the 2-layer cascade in the presence of nuclease enzymes showed that adding multiple layers of circuits to a system compounded the effect of nuclease degradation on the output values (Supplemental Figures 14 – 16). In all cases, a reduced conversion of input Initiator$_2$ strand concentration into detected Output concentration was observed, *i.e.*, there was a narrower range of initial [Initiator$_2$] that produced different levels of output fluorescence with a two-layer cascade than with a 1-layer cascade.

The model was able to predict the reduction in input:output conversion for 2-layer cascades with 2 bp for both layers or 5 bp (1st layer)/2 bp (2nd layer) toeholds observed in experiments, but experiments of 2-layer cascades with only 5 bp toeholds showed an even greater loss of input-to-output conversion than our model predicted (Supplemental Figure 14). Overall, the simulations suggest that circuit robustness decreases significantly with circuit depth, indicating that better methods of preventing degradation are needed to reliably operate more complex circuits, such as Boolean logic circuits.[6,7]

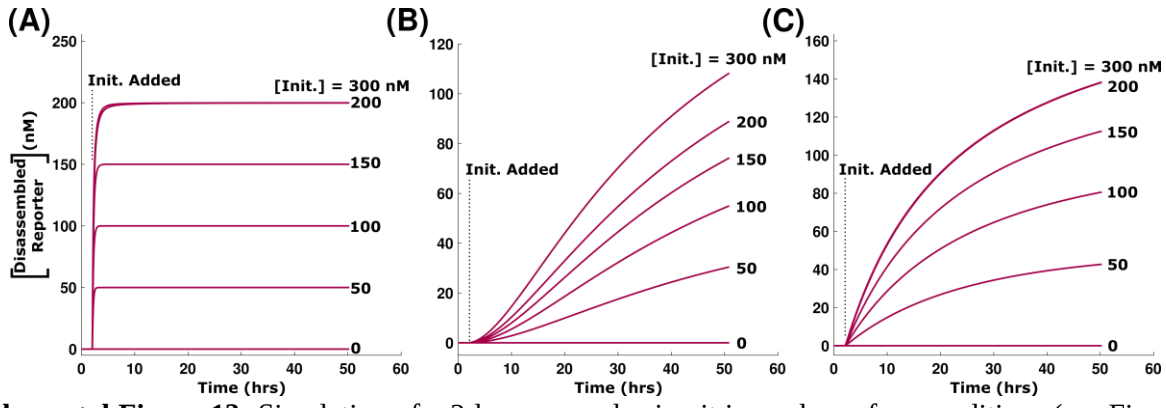

Supplemental Figure 13: Simulation of a 2-layer cascade circuit in nuclease-free conditions (see Figure 6a). (A) Simulated kinetics of a 2-layer cascade with 5 bp toeholds on both Source complexes in the cascade. (B) Simulated kinetics of a 2-layer cascade with 2 bp toeholds on both Source complexes in the cascade. (C) Simulated kinetics of a 2-layer cascade with a Source complex with a 5 bp toehold on the first layer and a 2 bp toehold on the second layer. Concentrations of reaction components are listed in Supplemental Table 7, except that all enzyme concentrations were set to zero. Reaction rate constants are listed in Supplemental Tables 1 – 6.

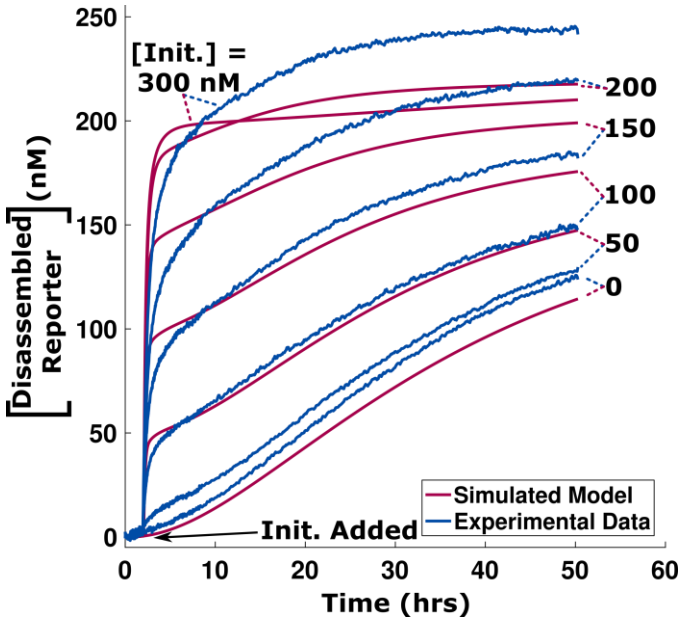

Supplemental Figure 14: Simulation of a 2-layer cascade with 5 bp toeholds on both Source complexes in the cascade in nuclease-screened medium. The concentrations of reaction components are listed in Supplemental Table 7. Experiments showed a slower initial rise of Disassembled Reporter signal upon addition of Initiator$_2$, suggesting less release of the final Output strand than experiments. There was also a lower range of initial [Initiator$_2$] that could be distinguished by final fluorescence than the model predicts.

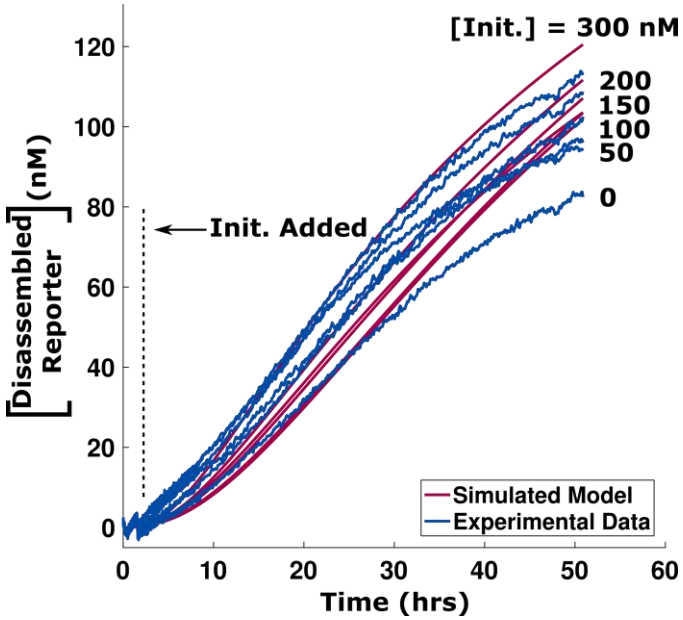

Supplemental Figure 15: Simulation of a 2-layer cascade with 2 bp toeholds on both Source complexes in the cascade in nuclease-screened medium. The concentrations of reaction components are listed in Supplemental Table 7. The simulations showed comparable Output strand release rates to what was observed in experiment. In general, it appeared that the release rate of the Output of the 2-layer cascade in this circuit, as measured by interaction with the Reporter complex, was dominated by degradation processes mediated by nucleases rather than by strand-displacement.

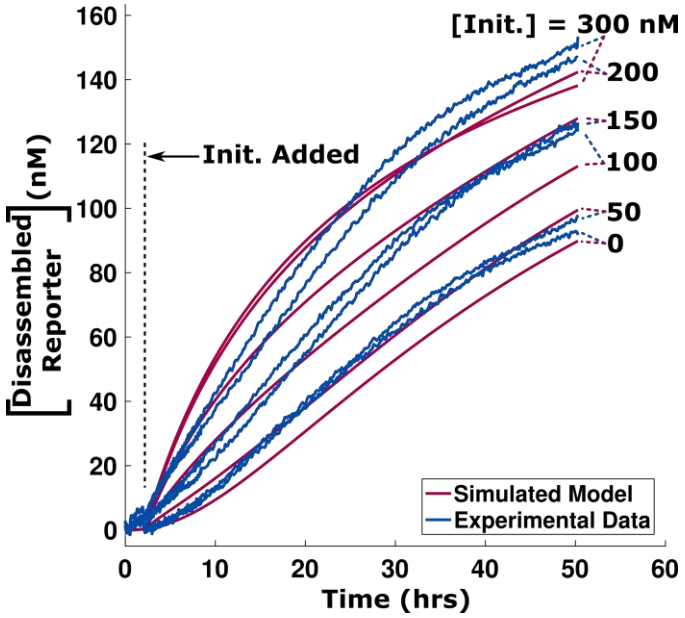

Supplemental Figure 16: Simulation of a 2-layer cascade with 5 bp toeholds on the first Source complex and 2 bp toeholds on the second Source complex in nuclease-screened medium. The concentrations of reaction components are listed in Supplemental Table 7. The simulations showed comparable Output strand release rates to what was observed in experiment. As in the 2-layer cascade in which both Source complexes had 2 bp toeholds, the release of Output appears to be largely directed by nuclease-mediated degradation.

SI 3.2: Timer circuits in nuclease-screened medium

To understand more about how circuits for controlled release might operate in serum-supplemented medium, we used a timer circuit which uses a slow release step coupled to a fast recapturing process to delay the overall production of the output species until the desired time.[5] When another process (*e.g.*, reporting, directing cellular behavior, or nanostructure assembly) is added downstream of the timer circuit, there is a competition between the downstream process and the recapturing process for the output species being slowly released. Thus, it is of interest to understand how degradation processes across all species influence the timing and competitive processes occurring within the timer circuit coupled to a downstream Reporter (Supplemental Figure 17), and to determine how well control over the timing of release can be achieved in serum.

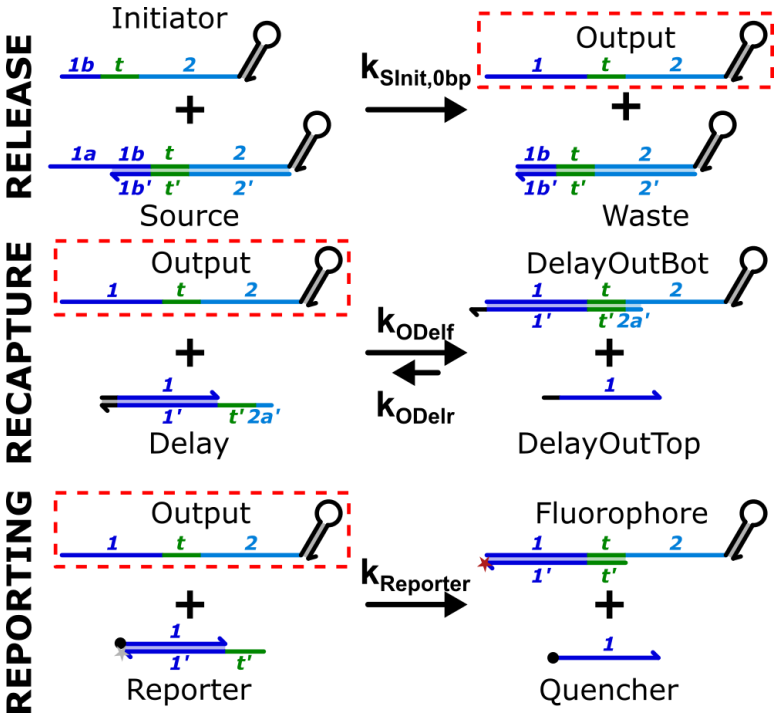

Supplemental Figure 17: Schematic of a timer circuit coupled to a downstream reporting process. The Output strand (red boxes) is slowly released from the Source complex using a 0 bp toehold initiation process. The Output can either be quickly recaptured using a Delay complex with a 7 bp toehold, or detected using a Reporter complex with a 5 bp toehold. The recapture process has a forward reaction rate constant ~20-fold larger than the reporting process.

To simulate the kinetics of the timer circuit in serum-supplemented medium, we constructed a model based on the ideas in SI 2, beginning with reaction equations 2 – 29. Reactions were then added to account for the added DNA circuit species, *Delay*, which was also assumed to be degraded by nucleases. Additionally, the following undesired "leak" reactions between the DNA components of the timer were also incorporated into the model as previously described[5] and as follows:

$$Output + Delay \xrightarrow{kODelf} DelOutTop + DelOutBot \quad (40)$$

$$DelOutTop + DelOutBot \xrightarrow{kODelr} Output + Delay \quad (41)$$

$$Source_{Leak} + Delay \xrightarrow{kS_{Leak}Del} OutDelBot_{Leak} + DelOutTop \quad (42)$$

$$Source + Delay \xrightarrow{kSDel} DelOutTop + DelOutBot \quad (43)$$

$$Delay + Enzyme \xrightarrow{kEDelf} Enzyme{:}\,Delay \quad (44)$$

$$Enzyme{:}\,Delay \xrightarrow{k_{EDelr}} Enzyme + Delay \quad (45)$$

$$Enzyme{:}\,Delay \xrightarrow{kEDelDeg} Enzyme + Waste \quad (46)$$

$$DelOutBot + Enzyme \xrightarrow{kEDelf} Enzyme{:}\,DelOutBot \quad (47)$$

$$Enzyme{:}\,DelOutBot \xrightarrow{k_{EDelr}} Enzyme + DelOutBot \quad (48)$$

$$Enzyme{:}\,DelOutBot \xrightarrow{k_{EDelDeg}} Enzyme + Output \quad (49)$$

$$Enzyme{:}\,DelOutBot \xrightarrow{k_{EDelDeg}} Enzyme + Waste \quad (50)$$

$$Initiator + Delay \xrightarrow{kInitDelf} Init{:}\,Del \quad (51)$$

$$Init{:}\,Del \xrightarrow{kInitDelr} Initiator + Delay \quad (52)$$

where *DelOutTop* and *DelOutBot* correspond to the top and bottom complex of the Delay/Output reaction. Reaction rate constants of the Delay-enzyme and DelOutBot-enzyme reactions were chosen to be the same as Reporter-enzyme reactions (SI 2.1). Equations 51 and 52 represent the reversible binding between Initiator and Delay complexes with reaction rate constants calculated as in Zhang and Winfree.[4] The off-rate k_{InitDelr} was calculated using "Nupack, dangles=some" parameters for a 7 bp toehold at 37 °C. The reaction rate constants in equations 40 – 43 were chosen as previously described[5] with minor adjustments made for reactions being conducted at 37 °C and in serum-supplemented medium (Supplemental Table 8). Reaction rate constants for Source degradation are listed in Supplemental Table 5 (no Initiator) and Supplemental Table 6 (with Initiator). Simulated component concentrations are listed in Supplemental Table 9.

Supplemental Table 8: Reaction rate constants for the simulation of the timer circuit as described in equations 40 – 52.

Rate Constant	Parameter Value
k_{ODelf} (1/M-sec)	$5x10^5$
k_{ODelr} (1/M-sec)	$5x10^1$
$k_{SLeakDel}$ (1/M-sec)	$2.5x10^4$
k_{SDel} (1/M-sec)	2.5
$k_{InitDelf}$ (1/M-sec)	$3.5x10^6$
$k_{InitDelr}$ (1/sec)	0.291

Supplemental Table 9: List of parameters used for simulating the reaction between Initiator and Source complexes in the timer circuit system incubated in serum-supplemented medium. The concentration of Reporter in the simulation was higher than the expected experimental concentration because the measured, calibrated concentration of Disassembled Reporter usually increased beyond the stoichiometric limit of the initial Reporter concentration in the experimental reaction mixture (Supplemental Note 2).

Reaction Component	Modeled Conc. (nM)	Expected Expt. Conc. (nM)
Reporter	250	200
Initiator	0 or 750	0 or 750
Source	750	750
Delay	0, 40, 80, 120, 160	0, 40, 80, 120, 160

As with the cascade circuit in SI 3.1, we characterized the effects of nuclease enzymes on the system by using the model to predict kinetics for the timer circuit with all enzyme concentrations set to zero (Supplemental Figure 18). Because downstream processes can compete with the Delay complex for released Output, we simulated the enzyme-free case in the presence of and without Reporter. When an irreversible Reporter is used to detect the release of Output from the timer circuit, it competes with the Delay complex for released Output strands to "load" the circuit and prevent the desired delayed-release behavior observed in the absence of Reporter complexes. This is in contrast to the reversible reporting used previously[5] that enabled Delay complexes to more favorably compete for released Output and kept the detected [Disassembled Reporter] low until the concentration of Delay complexes was effectively zero. Since reversible reporting requires continuous strand-displacement exchanges that keeps either a quencher-modified strand or the Output strand in a single-stranded form, the reporting process is more susceptible nuclease-mediated degradation that would disturb the process over time as an increasing amount of those single-stranded components are degraded.

In the presence of nucleases, Source complexes can degrade and release "active" Output molecules in the absence of Initiator, thus we considered both initiated and un-initiated cases

(Supplemental Figures 19 – 20). The timer circuit simulations show that while the model can reliably predict the behavior of the circuit, including the addition of an experimentally un-tested reaction component (Delay complex), the operability of the circuit is severely diminished due to the presence of the nucleases, again indicating the need for a more robust protection method. Experimental measurements of the system showed the same trends, but with an apparently lower Source degradation rate. This could be due to Delay complexes having a lower degradation rate than what was assumed.

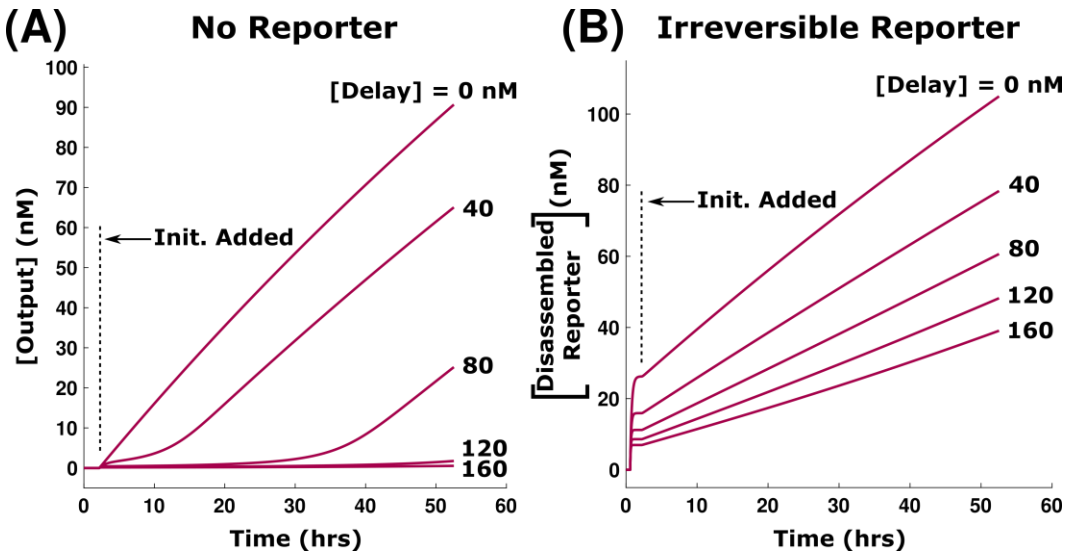

Supplemental Figure 18: Simulations of the release of Output in the timer circuit (Supplemental Figure 17) with all enzyme concentrations set to zero in the model. (A) Simulated kinetics of release of Output from the timer circuit without the Reporter complex. (B) Simulated kinetics of release of the Output from timer circuit measured using the irreversible Reporter. Concentrations of reaction components are listed in Supplemental Table 9, except that the concentration of all enzymes are set to zero. The Reporter competes with the Delay complex for released Output, loading the circuit, and preventing the delayed release behavior observed in (A).

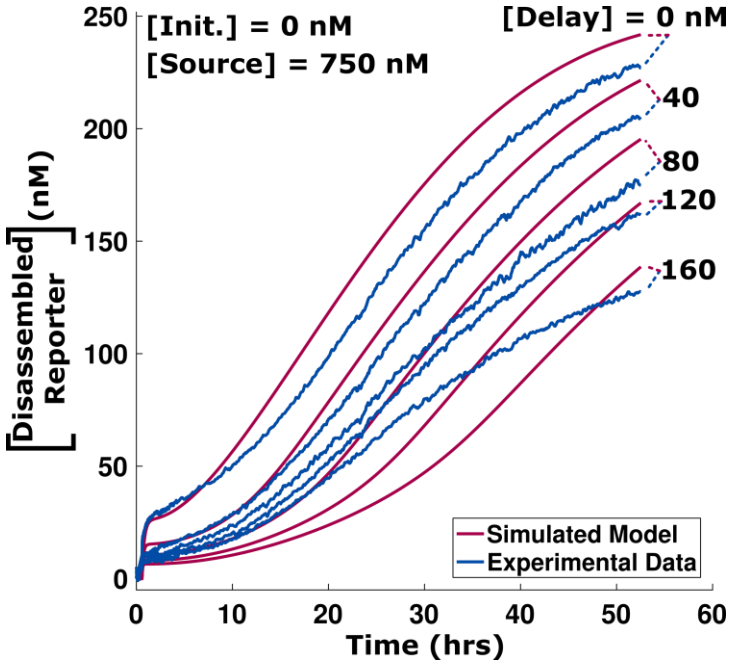

Supplemental Figure 19: Release of the timer circuit Output (as measured by its interaction with the Reporter complex) in the absence of Initiator. In this case, release is either a consequence of "leak" reactions, or degradation of the strand-displacement reaction components. Concentrations of reaction components are listed in Supplemental Table 9. Experiments and simulations show similar trends, although there is a longer lag time to release in simulations than in experiments.

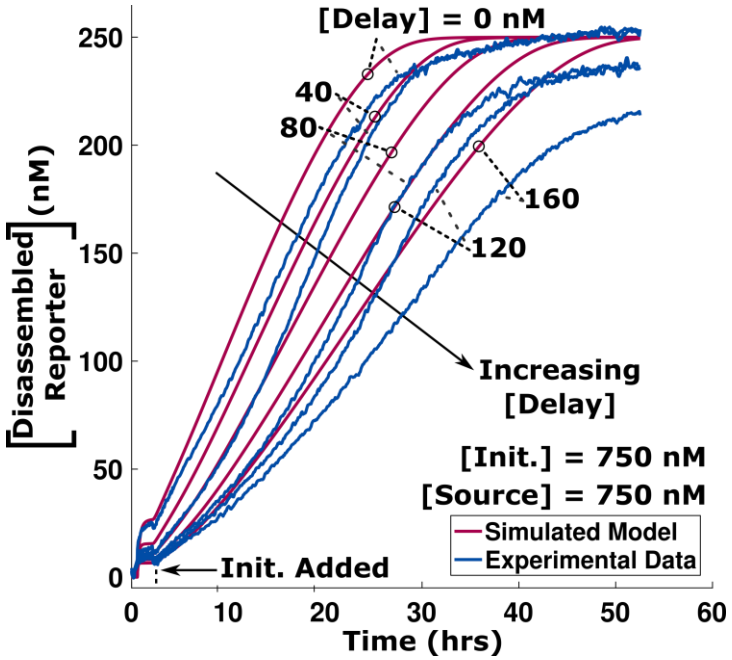

Supplemental Figure 20: Release of the timer circuit Output (as measured by its interaction with the Reporter complex) when Initiator in present. Concentrations of reaction components are listed in Supplemental Table 9. Experiments and simulations show similar trends. As noted above and in Supplemental Figure 18, delayed release is not observed due to Reporter complexes competing with Delay complexes for released Output (Supplementary Figure 17).

Supplemental Table 10: List of sequences and their names used in the experiments.

Strand Name	Role	Sequence
5' TOEHOLD REPORTER		
Rv(W5_)q	5'Rep1 IowaBlackFQ	/5IABkFQ/CA CCACCAAACTT CA
Rb(W5_)f	5'Rep1 FAM	TG AGA TG AAGTTTGGTGG TG/36-FAM/
W5_	5'Output, No Hairpin	CA CCACCAAACTT CA TCT CA
W5_6.extHP	5'Output, With Hairpin	CA CCACCAAACTT CA TCT CA TAACACAATCA CA CATCC TTTT GGATG
3' TOEHOLD REPORTER		
Rb5f	3'Rep1 IowaBlackFQ	/56-FAM/TG AAGTTTGGTGG TG AGA TG
Ro5Q	3'Rep1 FAM	CA CCACCAAACTT CA/3IABkFQ/
W_5	3'Output, No Hairpin	CA TCT CA CCACCAAACTT CA
Rb5f_extHP	3'Rep1 FAM, HP terminated	/56-FAM/TG AAGTTTGGTGG TG AGA TG CATCC TTTT GGATG
DECOY DNA		
W3prime_	Decoy DNA	AT AGATTTTAGGG AT CTC AT
W3_	Decoy DNA	AT CCCTAAAATCT AT CTC AT
PolyT20	Decoy DNA	TTTTTTTTTTTTTTTTTTTT
0 bp SOURCE PURIFICATION ADDITIVE		
W5(3)_6	S1.2 No Toehold	CTT CA TCT CA TAACACAATCA CA
RELEASE REACTION STRANDS		
W5_6.extHP	Source1.2 Top/Output	CA CCACCAAACTT CA TCT CA TAACACAATCA CA CATCC TTTT GGATG
Gb5(3)_6_5bp	5 bp Toehold Source1.2 Bottom	TG AGA TG TGATTGTGTTA TG AGA TG AAG
Gb5(3)_6_2bp	2 bp Toehold Source1.2 Bottom	GA TG TGATTGTGTTA TG AGA TG AAG
Gb5(3)_6_0bp	0 bp Toehold Source1.2 Bottom	TG TGATTGTGTTA TG AGA TG AAG
W5(3)_6_.extHP	Initiator1.2 5/2 bp Toeholds	CTT CA TCT CA TAACACAATCA CA TCT CA CATCC TTTT GGATG
W5(3)_6.extHP	Initiator1.2 0 bp Toehold	CTT CA TCT CA TAACACAATCA CA CATCC TTTT GGATG
2-LAYER CASCADE, SECOND LAYER		
W5(3)_6_7.extHP	Source1.2.3 Top	CTT CA TCT CA TAACACAATCA CA TCT CA ACATATCAATT CA CATCC TTTT GGATG
Gb6(3)_7_5bp	5 bp Toehold Source2.3 Bottom	TG AGA TG AATTGATATGT TG AGA TG TGA
Gb6(3)_7_2bp	2 bp Toehold Source2.3 Bottom	GA TG AATTGATATGT TG AGA TG TGA
W6(3)_7_.extHP	Initiator2.3	TCA CA TCT CA ACATATCAATT CA TCT CA CATCC TTTT GGATG
TIMER CIRCUIT		
W5(3)_6.extHP	Initiator1.2 0 bp Toehold	CTT CA TCT CA TAACACAATCA CA CATCC TTTT GGATG
W5_6.extHP	Source1.2 Top/Output	CA CCACCAAACTT CA TCT CA TAACACAATCA CA CATCC TTTT GGATG
Gb5(3)_6_0bp	0 bp Toehold Source1.2 Bottom	TG TGATTGTGTTA TG AGA TG AAG
Tv5	Delay1 Top	CT CA CCACCAAACTT CA
Tb5	Delay1 Bottom	TA TG AGA TG AAGTTTGGTGG TG AG

SI References

1. Matsuno, H., Furusawa, H., and Okahata, Y. (2005) Kinetic studies of DNA cleavage reactions catalyzed by an ATP-dependent deoxyribonuclease on a 27-MHz quartz-crystal microbalance. *Biochemistry 44*, 2262-2270.
2. Mannherz, H. G., Goody, R. S., Konrad, M., and Nowak, E. (1980) The interaction of bovine pancreatic deoxyribonuclease I and skeletal muscle actin. *Eur. J. Biochem. 104*, 367-379.
3. Eder, P. S., Rene, R. J., Dagle, J. M., and Walder, J. A. (1991) Substrate specificity and kinetics of degradation of antisense oligonucleotides by a 3' exonuclease in plasma. *Antisense Res. Dev. 1*, 141-151.
4. Zhang, D. Y., and Winfree, E. (2009) Control of DNA strand displacement kinetics using toehold exchange. *J. Am. Chem. Soc. 131*, 17303–14.
5. Fern, J. Scalise, D., Cangialosi, A., Howie, D., Potters, L., and Schulman, R. (2016) DNA strand-displacement timer circuits. *ACS Synth. Biol. 6*, 190-3.
6. Seelig, G., Soloveichik, D., Zhang, D. Y., and Winfree, E. (2006) Enzyme-free nucleic acid logic circuits. *Science 314*, 1585–8.
7. Qian, L., and Winfree, E. (2011) Scaling up digital circuit computation with DNA strand displacement cascades. *Science 332*, 1196–201.